Thermal Pyranometer Using the Open Hardware Arduino Platform

Elson Avallone*[(1)(2)], Paulo César Mioralli[(1)(2)], Vicente Luiz Scalon[(2)], Alcides Padilha[(2)], Santiago del Rio Oliveira[(2)]

[(1)] Instituto Federal de Educação, Ciência e Tecnologia de São Paulo, Av. Pastor José Dutra de Moraes, 239, Câmpus 15808-305-Catanduva-SP, Brazil

[(2)] UNESP - Univ Estadual Paulista, Faculdade de Engenharia, Departamento de Engenharia Mecânica, Av. Eng. Luiz Edmundo C. Coube 14-01, Bauru, SP, Brazil

E-mail: [1]elson.avallone@yahoo.com.br

Abstract

Thermal Pyranometers are very important devices for evaluating the intensity of solar radiation under different climatic conditions. These devices utilize thermal radiation for comparison and determination of their efficiency. Because of this wide use associated with the development of new technologies, a simple and low-cost version of thermal pyranometer has been studied, designed and manufactured. A blackened aluminum disk is used as a hot junction, and the cold junction is exposed to ambient air. The two terminals are connected to a digital amplifier with output signal directed to an Arduino board. A device calibration was performed by comparing the results with a commercial photodiode sensor. Statistical analysis of the calibration data considering a 99% confidence level leads to an estimated standard error of 20.8 W/m². An analysis of its response time also estimated from a dynamic model. This model uses a numerical solution of the energy balance on heat exchange between the aluminum disc and the environment. The instrument response time based on the average of the estimates obtained from the dynamic model is about 1.5 minutes. Based on these studies it was concluded that the characteristics of the sensor are adequate for most solar energy tests and the final cost of US $ 60.00 is much lower than the large majority of such commercial devices.

Keywords: Pyranometer; Radiometer; Thermal sensor; Arduino.

1. Introduction

Pyranometers are sensors used for measurements of the intensity of solar radiation [W/m^2]. There two main types of pyranometers, with the optical sensor type using a photodiode, which produces microvolt signals and uses an amplifier circuit [1,2]. The influence of a silicon solar cell with spectral response in the measurement of solar radiation was studied by [1]. The construction of a photodiode pyranometer was performed by [3]**,** using the calibration procedure described in [4] and tested in the laboratory by [5]**,** who used artificial lighting and photovoltaic sensors. A sensor using the BPW21 photodiode with operational amplifier was built and calibrated by [6] using the standards [7,8]. A pyranometer solar cell was developed by [9]and also calibrated by the standards [10,11]. A teflon diffuser was studied in [12] to avoid saturation and [13] calculated the calibration constant using a thermal sensor.

Several researchers [14,15] constructed a pyranometer using "K" junctions while [16] used 2 LM35DZ analog sensors for differential temperature measurements. [17] Installed a "T" junction on the outer surface of a solar collector by evacuated pipe where the temperature profile is similar to a commercial thermal pyranometer.

The use of thermal pyranometer has the advanted of capturing thermal radiation in the same wavelengths as a solar collector. This effect does not happen with radiation sensors based on photodiodes.

2. Mathematical Modeling

Based on the principle observed by [17], a thermal sensor was studied with the analogous operation of a flat plate solar collector as shown in Figure 1.
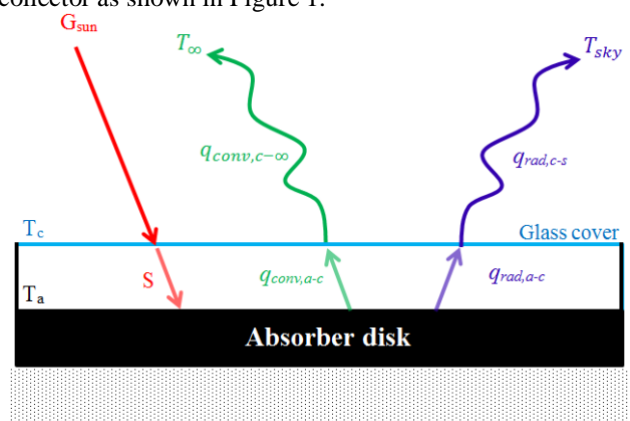

Figure 1. Schematic drawing of the thermal sensor depicting the energy conservation on the absorber disk.

To evaluate the response time of the direct radiation sensor due to the physical parameters, a mathematical model was used assuming a blackened disk with small mass "m", and under conditions of direct sunlight. Eq. (1) describes the simplified transient heat conduction for one-dimensional analysis, subject to initial conditions, such that the temperature of the absorber disk (T_a) is equal to the initial temperature, i.e., $t = 0 \rightarrow T_a = T_\infty$, which results in

$$m.c_p.\frac{dT_a}{dt} = S - q_{conv,a-c} - q_{rad,a-c} \tag{1}$$

where c_p is the specific heat at constant pressure and S is the effective irradiation reaching the absorber.

In Eq. (2), the heat flow can be obtained from the ambient radiation as function of transmittance (τ), absorbtance (α) and the global flow (G_{sun}):

$$S = (\tau.\alpha).G_{sun} \tag{2}$$

From Eq. (3), the cover glass temperature and energy balance are obtained for steady state conditions as:

$$q_{conv,a-c} + q_{rad,a-c} = q_{conv,c-\infty} + q_{rad,c-s} \tag{3}$$

where $q_{conv,a-c}$ is the convective heat flow between the absorber and the cover glass, $q_{rad,a-c}$, the heat flow by irradiation between the absorber and the cover glass, $q_{conv,c-\infty}$ the convective heat flow between the cover and the ambient air and $q_{rad,c-s}$ the heat flow by irradiation between the cover and the sky.

The determination of the convective heat transfer rates can be obtained if the glass temperature is known, which in turn is obtained from the energy balance equation (Eq. 3). Several authors discuss the best way to estimate heat transfer rates, highlighting [18–20].

2.1 Radiation Heat Flow Between the Sky and the Cover Glass of the Pyranometer

The heat exchange radiation, i.e., the net heat flow, is proportional to the difference between the fourth power of the temperatures. In this case, using the *Stefan-Boltzmann* to a grey surface, it follows that:

$$q''_{rad,c-s} = \varepsilon_c.\sigma.\left(T_a^4 - T_{sky}^4\right) \tag{4}$$

where the sky temperature (T_{sky}) can be calculated by the empirical Eq. (5) proposed by [21] based on the dew temperature (T_{dew}), dry bulb ambient temperature (T_∞) and time of day (t):

$$\begin{aligned} T_{Sky} = T_\infty.[0,711 &+ 56 \times 10^{-4} \times T_{dew} \\ &+ 73 \times 10^{-6} \times T_{dew}^2 \\ &+ 13 \times 10^{-3} \times \cos(15t)]^{1/4} \end{aligned} \tag{5}$$

where: T_∞ is the ambient temperature and T_{dew} is the dew temperature, both in degrees Celsius [°C]. However, for purpose of this study, the sky temperature (T_{sky}) is assumed to be 2.5°C above ambient temperature during the daytime, therefore Eq. (5) is not necessary.

2.2 Radiation Heat Flow Between the Absorber Disk and the Cover Glass

For this study, heat exchange occurs between two gray surfaces. Thus, the equation for heat exchange by radiation is slightly modified and involves the emissivity of the two surfaces and is described by:

$$q''_{rad,a-c} = \frac{\sigma.(T_a^4 - T_c^4)}{\frac{1}{\varepsilon_c} + \frac{1}{\varepsilon_a} - 1} \tag{6}$$

where T_a and T_c are the temperatures of the absorber disk and the cover glass, and ε_c and ε_a are the emissivity of the cover glass and absorber, respectively.

2.3 Convection Heat Flow Between the Sky and Cover Glass

The heat exchange by convection between the cover glass and the ambient air can be obtained through empirical equations. As the collector is usually exposed in an open area, wind velocity plays a fundamental role. Thus, Duffie and Beckman [18] proposes the use of *Sparrow* expression given in Eq. (7) adapted to calculate a heat transfer coefficient and Lc, which in this case is d/4, valid for the range $10^4 < Re < 4.5 \times 10^4$

$$\overline{Nu_{Lc}} = 1.72 \cdot Re^{1/2} \cdot Pr^{1/3} \tag{7}$$

where $L_c = A_a/P_a$ is the spacing between the cover glass and the absorber disk, A_a is the surface area of the disk and P_a is the disk perimeter. Based on the definition of the Nusselt number (Nu), the heat transfer coefficient can be obtained, and hence the convective heat flow of the cover glass to the sky ($q''_{conv,c-\infty}$).

2.4 Convection Heat Flow Between the Absorber and the Glass Cover

The movement of air between the absorber disk and the glass induces a natural movement in this cavity, with inclination θ, and [18] have suggested the use of Eq. (8) [22]:

$$\begin{aligned} \overline{Nu_{Lc}} = 1 + 1.44 \cdot &\left\{1 - \frac{1708[sin(1.8 \cdot \theta)]^{1.6}}{Ra_{Lc} \cdot cos\theta}\right\} \\ &\cdot \left[1 - \frac{1708}{Ra_{Lc} \cdot cos\theta}\right] \\ &+ \left[\left(\frac{Ra_{Lc} \cdot cos\theta}{5830}\right)^{1/3} - 1\right] \end{aligned} \tag{8}$$

This expression is suitable for most collectors. It requires that the ratio of the height of the collector and the spacing between the cover glass and the collector (H/L_c) be higher than 12. The heat transfer coefficient obtained from Eq. (8) allows the evaluation of the heat exchange by Newton's Law of Cooling using ($T_a - T_c$) as the temperature difference. A detailed expression is given by [23].

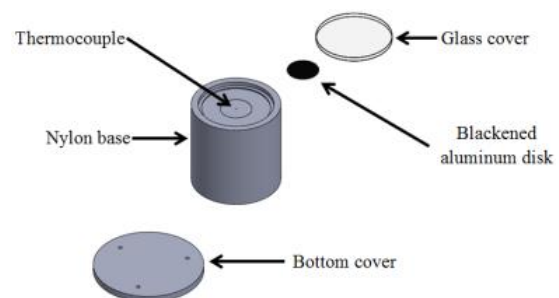## 3. Design and Manufacturing of the Pyranometer

Figure 2. Exploded perspective of the pyranometer.

Based on the mathematical model a pyranometer was manufactured to measure the solar radiation in a small blackened aluminum disk with 20mm diameter and 0.1mm thickness (Figure 2), which behaves as a flat plate solar collector. A "K" junction is fixed to the lower surface of the disc to measure the "hot" temperature (T_a), i.e., hot source. A second junction measures the "cold" temperature T_∞, i.e., ambient temperature. The connection between the junctions, shown in Figure 3, registered the voltage difference between these junctions.
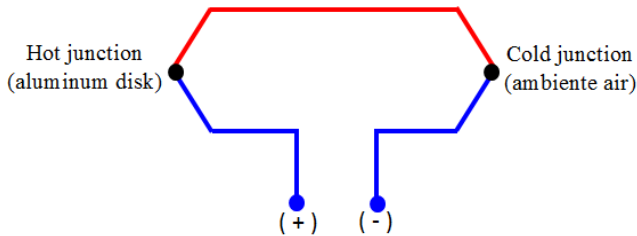

Figure 3.Connection between junctions.
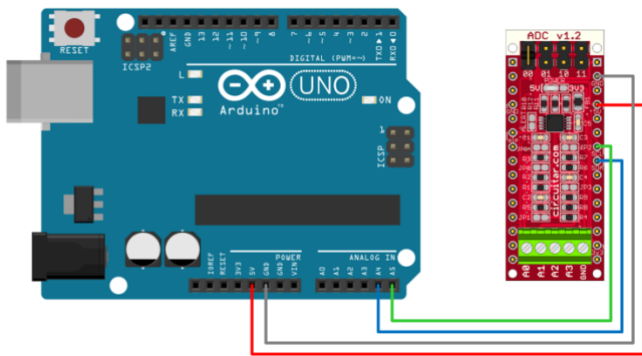

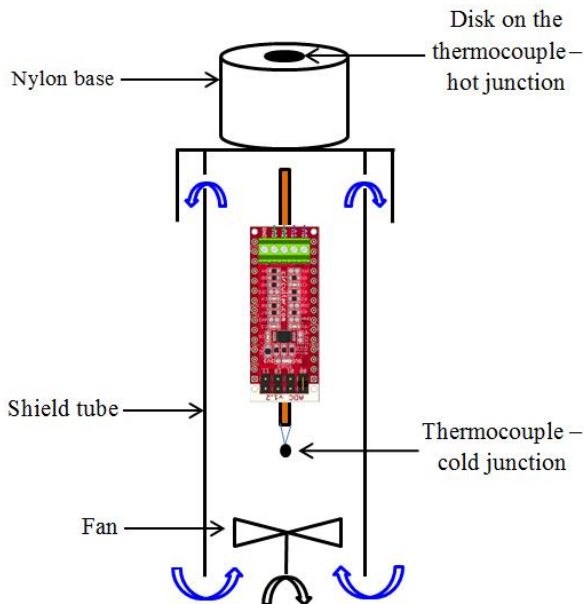Figure 4. Connection between the ADS1115x converter and Arduino UNO board.

Figure 5.Pyranometer assembly with cooling system.

As the signal generated by the junctions is in millivolts (mV), an amplifier for reading the voltage between the terminals is required. These terminals are connected to an amplifier analog-to-digital converter (model ADS1115) where the (+) terminal is connected to the analog port A2 and (-) to the port A3 of the Arduino board, as shown in Figure 4. The gain of the analog-to-digital converter is controlled by a programming parameter defined by the manufacturer. In this work, the gain is 16x, i.e., the largest available. To avoid overheating of the ADS1115 converter, it was necessary to install a cooling system.

The ventilation system sucks air through the lower region of the instrument, resulting in cooling of the cold junction and of the ADS1115. Warm air is then blown out through ventilation holes, as shown in Figure 5.

The pyranometer calibration was performed at IPMet (Meteorological Research Institute - UNESP-Bauru), installing the pyranometer beside a photodiode sensor (Campbell Scientific Inc., model LI200X) for comparison of the signals. The assembly is shown in Figure 6.

Figure 6. Assembly of the pyranometer beside a photodiode sensor (Campbell Scientific Inc., model LI200X) for comparison of the signals.

4. Results and Discussions

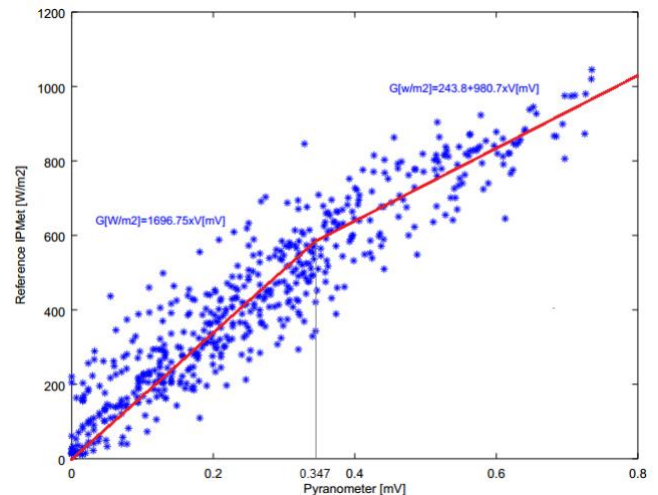For calibration, the point cloud for the two devices was generated, and is shown in Figure 7.

Figure 7. Cloud points used for calibration of the pyranometer.

Based on the date analisys, a bilinear approximation was chosen. The transition point between the two regions was obtained as to optimise the correlation coefficient.

For better reliability of the calibration, two average linear trends were generated: one in the range 0 - 0.347mV (Eq. 9) and another in the range 0.347 - 0.8mV (Eq. 10).

$$G_{1\left[\frac{W}{m^2}\right]} = 1696.75 \times V \tag{9}$$

$$G_{2\left[\frac{W}{m^2}\right]} = 243.8 + 980.7 \times V \tag{10}$$

where V is given in [mV

Eqs. (9-10) were introduced in an Arduino sketch, making it possible to scan all the instrument spectrum. The standard error for the LI200X photodiode sensor is 4.35 W/m².

The radiation curves of the pyranometer and the photodiode sensor are shown in Figure 8. The x-axis shows time in hours from zero-hour of the first day of the year.
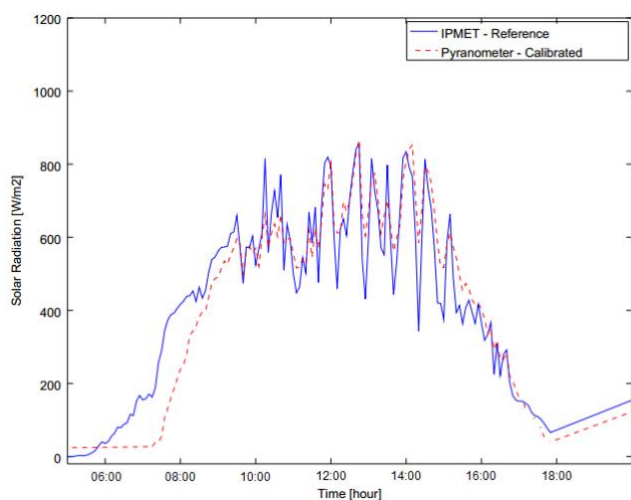

Figure 8.Calibration curve.

Earlier in the day (06:00), in Figure 8, the aluminum disk was at a temperature considered low, due to the heat loss at night. Upon receiving the sunlight, (07:00-09:00), the pyranometer has a longer response time than the photodiode. From 09:00, the instruments have smaller difference between measures, and this happens after the aluminum disk achieves steady state thermal regime.

At the end of the day (15:00-18:00), the pyranometer has a similar behavior to the photodiode equipment, with its faster response time. Also, the solar radiation capture angle to the zenith is greater in the photodiode. The pyranometer, in turn, captures solar radiation analogously to the solar collector, and tends to become closer to the effectively measured radiation. As the instruments operate with different principles, a small difference between them is expected. Despite this, the calibration curve showed a small dispersion of experimental points and a low error value calculated to a confidence level of 99%, according to the simulation with the GNU OCTAVE software. This also contributed to the large number of experimental points used.

Based on the mathematical model described, Scalon and Oliveira [24] analyzed the pyranometer behavior and tested the equipment response time, using the GNU OCTAVE software for the simulation.

For simulations, from initial temperature of the absorver of 3°C, the pyrnometer response time is approximately 2.5 minutes to reach the equilibrium temperature. As the initial temperature increases, the response time decreases. Increasing the initial temperature to 33°C, the time for equilibrium is approximately 1.5 minutes.

5. Conclusions

The thermal sensor studied proved reliable, considering the data obtained in the calibration and the verified standard error of 20.8W/m². This value is adequate for most measurements of heat flow by radiation in tests involving solar collectors.

The response time is also suitable for these tests, estimated at about 1.5 minutes. On the use in water heating with solar energy, this time is appropriate because the heat transfer to the water is also a slow process.

The equipment has a good cost-benefit ratio, since its cost is under US$ 60.00. Another important advantage is the use of Arduino platform that is able to record large amounts of data, eliminating the need of a data logger, aiding in reducing the final cost of the equipment.

References

[1] I. Zanesco and A. Krezinger, "On the threshold of the accuracy of using silicon solar cells to measure global solar irradiance," in *11th Photovoltaic energy conference, Montreux Swizerland*, Montreux - Suíça, 1992.

[2] S. Awasthi, A. Dubey, J. M. Kellar, and O. Mor, "Design and simulation of eletronic instruments for solar energy measurement system," *Int. J. Sci. & Eng. Res.*, 3, 1, Jan-2012.

[3] H. Vera Luiz, A. J. Busso, and F. Benitez, "Piranómetro fotovoltaico con sistem autónomo de adquisición de datos," *Avances en Energías Renovables y Medio Ambiente*, 9, 2005.

[4] I. Zanesco, "Analise e Construçao de um Piranômetro Fotovoltaico," Dissertação de Mestrado, Universidade Federal do Rio Grande do Sul, Porto Alegre, 1991.

[5] M. A. Martínez, J. M. Andújar, and J. M. Enrique, "A new inexpensive pyranometer for the visible spectral range," *Sensors*, 9, 4615–4634, 2009.

[6] D. W. Medugu, F. W. Burari, and A. A. Abdulazeez, "Construction of a reliable model pyranometer for irradiance measurements," *African Journal of Biotechnology*, 9, 1719–1725, 2010.

[7] ISO 9847, *Solar Energy — Calibration of field pyranometer by comparison to a reference pyranometer*. 2013.

[8] ISO 9060, *Standard & Pyranometer Measurement Accuracy*. 2012.

[9] W. A. Vilela, "Estudo, desenvolvimento e caracterização de radiômetros para medição da raciação solar," Tese de Doutorado, Instituto Nacional de Pesquisas Espaciais - INPE, São José dos Campos - SP, 2010.

[10] WMM, "Instruments and observing methodos - Report Nº 98." World Meteorological Organization, 2009.

[11] M. et al Krazenerg, "Rastreabilidade de radiômetros para medida da energia solar," in *Meteorologia 2003 - Meteorologia para a vida*, Recife - PE, 2006.

[12] M. A. M. Bohórquez, J. M. E. Gómez, E. D. Aranda, M. J. V. Vázquez, and J. M. A. Márquez, "Sistema de instrumentación de bajo coste para la medición de irradiancia en el rango espectral visible," in *XXXII*

Jornadas de Automática, Sevilla - Espanha, 1, 2011. 1.

[13] S. N. Nwankowo, M. N. Nnabuchi, and J. E. Ekpe, "Construction and characterization of a pyranometer using locally avaliable materials for global solar radiation measurement," *Asian Transactions on Basic and Applied Sciences*, 2, 2012.

[14] J. L. Souza and J. F. Escobedo, "Construção de um saldo radiômetro com termopilha de filme fino e avaliação de sua performance," *Revista Brasileira de Meteorologia*, 10, 29–36, 1995.

[15] J. F. Escobedo, V. A. Frisina, R. P. Ricieri, and A. P. Oliveira, "Radiômetros solares com termopilhas de filmes finos - I Descrição e custos," *Revista Brasileira de Aplicações de Vácuo*, 16,, 1997.

[16] J. M. Gomes, P. M. Ferreira, and A. E. Ruano, "Implementation of an intelligent sensor for measurement and prediction of solar radiation and atmospheric temperature," in *Sensors Journal, IEEE*, Floriana - Malta, 2011, 1–6.

[17] E. Avallone, "Avaliação da Eficiência Térmica de um Coletor Solar Tipo Tubo Evacuado Modificado," Master Thesis, Universidade Estadual Paulista - Júlio de Mesquita Filho, Campus de Bauru, 2013.

[18] J. A. Duffie and W. A. Beckman, *Solar Engineering of Thermal Process*, 4ª., vol. 1. USA: John Wiley & Sons, 2013.

[19] S. A. Kalogirou, "Solar thermal collectors and applications," *Progress in Energy and Combustion Science*, 30, 231–295, 2004.

[20] S. A. Kalogirou, *Solar Energy Engineering*, 1ª., vol. 1. United States of America: British Library Cataloguing-in-Publication, 2009.

[21] P. Berdahl and M. Martin, "Emissivity of clear skies," *Solar Energy*, vol. 32, no. 5, p. 663, 1984.

[22] K. G. T. Hollands, T. E. Unny, G. D. Raitby, and L. Konieck, "Free convection heat transfer across inclined air layers," *Trans ASME J. Heat Transfer*, 98, 1976.

[23] F. P. Incropera, D. P. Dewit, T. I. Bergman, and A. S. Lavine, *Fundamentos de transferência de calor e massa*, 6th ed., vol. 1, 1 vols. Rio de Janeiro: LTC - Livros técnicos e científicos Editora Ltda, 2008.

[24] V. L. Scalon and S. D. R. Oliveira, "*Theoretical analysis of a flat pyranometer*," presented at the VII SiAT - Simpósio de Análise Térmica, Universidade Estadual Paulista "Júlio de Mesquita Filho," 4, 2015.